ORIGINAL PAPER

Effect of high valency cations on the (BiPb)$_2$Sr$_2$Ca$_3$Cu$_4$O$_{12+\delta}$ compounds

Duygu Yazici · Bekir Ozcelik

Abstract We have produced the (BiPb)$_2$V$_x$Sr$_2$Ca$_3$Cu$_{4-y}$-Ti$_y$O$_{12+\delta}$ compounds by a melt-quenching method. For two different sintering times (185 and 192 hours), the effects of vanadium adding and Ti doping on the structure have been investigated by electrical resistance, scanning electron micrographs (SEM), XRD patterns and magnetic hysteresis loop measurements. It has been found that the high-T_c superconducting phase, (2223), is formed in the samples annealed at 845 °C for 185 and 192 h, with concentration $x = 0.2$ and $y = 0.05$. However, with increasing Ti doping the (2223) phase gradually transforms into the (2212) phase. The hysteresis loop areas decrease with increasing Ti concentration and sintering time. Our data have indicated that the critical current, J_c, decreases with increasing magnetic field.

Keywords Bi-based cuprates · Critical currents · Magnetic properties

1 Introduction

It is well known that the superconductivity is suppressed by the presence of magnetic ions in conventional metallic superconductors. This phenomenon can be understood in terms of the pair-breaking mechanism. On the other hand, the existence of some magnetic rare-earth metallic superconductors has been explained by claiming that the superconductivity and the magnetism take place in different parts of the crystal, with little interaction between the two. However, in all high-T_c ceramic superconductors, the CuO$_2$ planes which contain magnetic Cu^{2+} ions, which probably enhance the superconductivity, instead of degrading [1].

Weak coupling between BiO–BiO layers in the BSCCO system enables the substitution of the different oxides for Bi^{3+} site. Some of the results have demonstrated that there is no significant increase in the T_c. But important changes occur in the carrier concentration due to the different cation doping levels. Therefore, the electrical property of the system varies. Here we should state that the preparation technique of a system is also very important. To this end preparing the BSCCO system by the glass-ceramic technique yields good density and minimum porosity, compared to the conventional solid state technique [2–4].

Tarascon et al. [5], studied various substitutions of the rare-earths into the Bi$_4$Sr$_4$Ca$_{2-x}$R$_x$Cu$_4$O$_y$ ($x \geq 1$) and reported that for $x = 1.5$ the compounds became semiconducting. At low doping ($x \leq 0.5$) T_c was not much affected. They further found that the depression of T_c occurred no matter whether the dopand was magnetic or non-magnetic, and that the superconducting properties were strongly affected by changes in the hole concentration, induced by the amount of doping.

The formation of pure and textured (2223) phase is a critical issue in fabricating BSCCO superconductors. Since the reaction kinetics of the Bi-(2223) phase formation is very slow, long periods of sintering at temperatures close to its decomposition temperature are required [6]. Many factors, including composition, phase assemblage of the precursor powder, lead content, grain alignment, intergrain connectivity, density of the core, sintering parameters and doped ions, significantly influence the heat treatment parameters and final physical properties of the samples [7]. T_c of superconducting copper oxide based compounds depends on the density of mobile holes in the CuO$_2$ planes and thus on the average Cu valency [8].

D. Yazici (✉) · B. Ozcelik
Department of Physics, Faculty of Sciences and Letters,
Çukurova University, 01330 Adana, Turkey
e-mail: yazici.dyg@gmail.com

Partial substitution of Pb for Bi has been found to favor the growth of the (2223) phase, i.e., it has been observed that the (2223) phase can be made more stable by doping a small amount of Pb [9–11]. The nominal composition of Pb was determined as 0.4 atomic percent [12, 13]. It was also reported that Pb atoms behave as efficient nucleation and growth sites for the formation of 2223 phase and enhance the diffusion of the calcium and copper atoms [14–16]. With heat treatment under carefully controlled conditions, the material consisting of single (2223) phase can be prepared as evidenced by sharp T_c at 110 K. For these samples electron microscopic investigations show that Pb^{2+} ions exclusively replace Bi^{3+} ions in the lattice.

As stated in the previous paragraph it has now been well established that the superconducting properties of the copper oxide superconductors are related to the hole concentration. Nevertheless, there are few reports on the effects of substitutions to Cu sites in the BSCCO (2223) system. It is recently observed that niobium, vanadium, and titanium addition increases the (2223) phase considerably and succeeded to isolate this phase up to 96% and 97% [17, 18]. In this study, we desire to investigate both the effect of the sintering time on the formation of the high T_c phase and the effect of other high valency cations like vanadium and titanium.

2 Experimental Process

The appropriate amounts of Bi_2O_3, PbO, TiO_2, V_2O_5, $SrCO_3$, $CaCO_3$, and CuO fine powders in the stoichiometric ratios of $Bi_{1.6}Pb_{0.4}V_xSr_2Ca_3Cu_{4-y}Ti_yO_{12+\delta}$ ($x = 0.2$ and $y = 0.05$ and 0.10) were well mixed by milling and calcined at 750 °C for 24 h in air. The mixture was re-ground about one an half hour and the resulting powder was placed in a platinum crucible and heated at 1200 °C until the samples were completely melted. The melts were poured onto a pre-cooled copper plate and pressed quickly by another copper plate to obtain an approximately 1.5 to 2 mm thick plate like amorphous (glass) material. The mixture was re-grinded for about two hours and the resulting powder were then pressed into pellets of 13 mm diameter by applying a 5 tons pressure. Finally, the precursor materials produced were sintered at 845 °C for 185 h and 192 h in air to achieve crystallized material and superconductivity. The samples sintered 185 hours, with $x = 0.2$ and $y = 0.05$ and 0.10 will be hereafter named as A, B, respectively. The samples sintered 192 h, having the same nominal composition with A, B will be hereafter named as A1 and B1, respectively.

Resistivity measurements were carried out on our samples using a standard four-probe method with silver paint contact. X-ray powder diffraction analyses were performed by using Rigaku RadB powder diffractometer system with $CuK\alpha$ radiation and a constant scan rate between $2\theta = 3–60°$ at room temperature, to examine the phases present
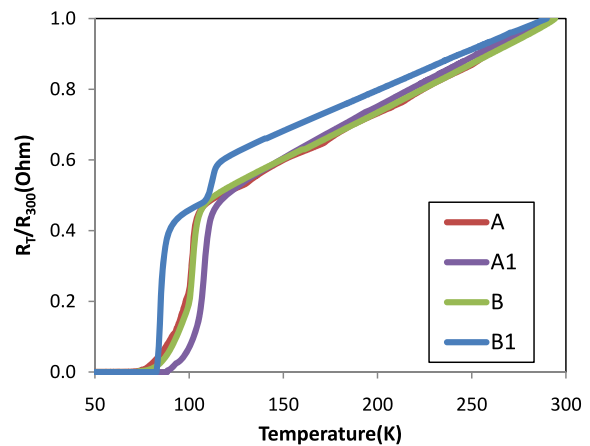

Fig. 1 (Color online) Temperature dependence of resistivity for the samples *A*, *B*, *A1* and *B1*

in the samples. SEM photographs for the study of the microstructure were taken by using a LEO Evo-40 VPX scanning electron microscope (SEM) and Röntec energy dispersive X-ray spectroscopy (EDX). The magnetic measurements were performed with a 7304 model Lake Shore VSM.

3 Results and Discussions

The normalized resistance to room temperature of the samples A, B, A1 and B1 are presented in Fig. 1. For the samples A and B although the $T_{c.onset}$ (below which the sample is in a superconducting state) of superconductivity are about 102 K, R almost goes to zero at $T_{c.offset} = 83$ K. Hence, the superconducting transition range ΔT of about 19 K, indicates that the high-T_c phase (2223) is not the dominant phase and (2212) phase is fall into with (2223) phase in the samples. Samples A and B show almost the same characteristic curves near the zero resistance temperatures and their normal states. On the other hand, for the sample A1 the $T_{c.onset}$ of superconductivity are about 113 K, the $T_{c.offset} = 100$ K and ΔT of about 13 K indicating the high-T_c phase (2223) is the dominant phase. But the general behavior of sample B1 is completely different from sample B. It was found that the resistance of sample B1 decreases with temperature in the normal state, and shows two onset transition temperature at the temperatures of 113 and 91 K; it then drops sharply to zero at $T_{c.offset} = 82$ K. This behavior indicates that the sample has two phases, namely (2223) and (2212). As a result our resistance measurements have shown that the increase in Ti concentration and sintering temperature causes a broadening transition and a decrease of the $T_{c.offset}$ values.

The XRD diffraction patterns of A, B, A1 and B1 samples are shown in Fig. 2. The X-ray diffractometry results of the samples A and B show both the (2223) and (2212) structure. On the other hand for samples A1 and B1 besides two

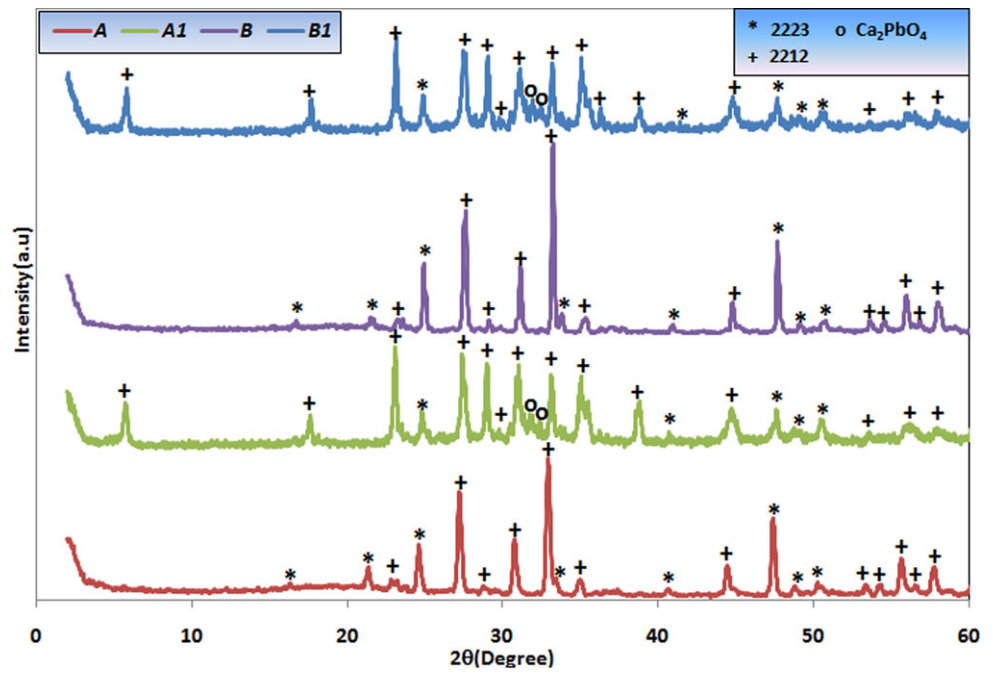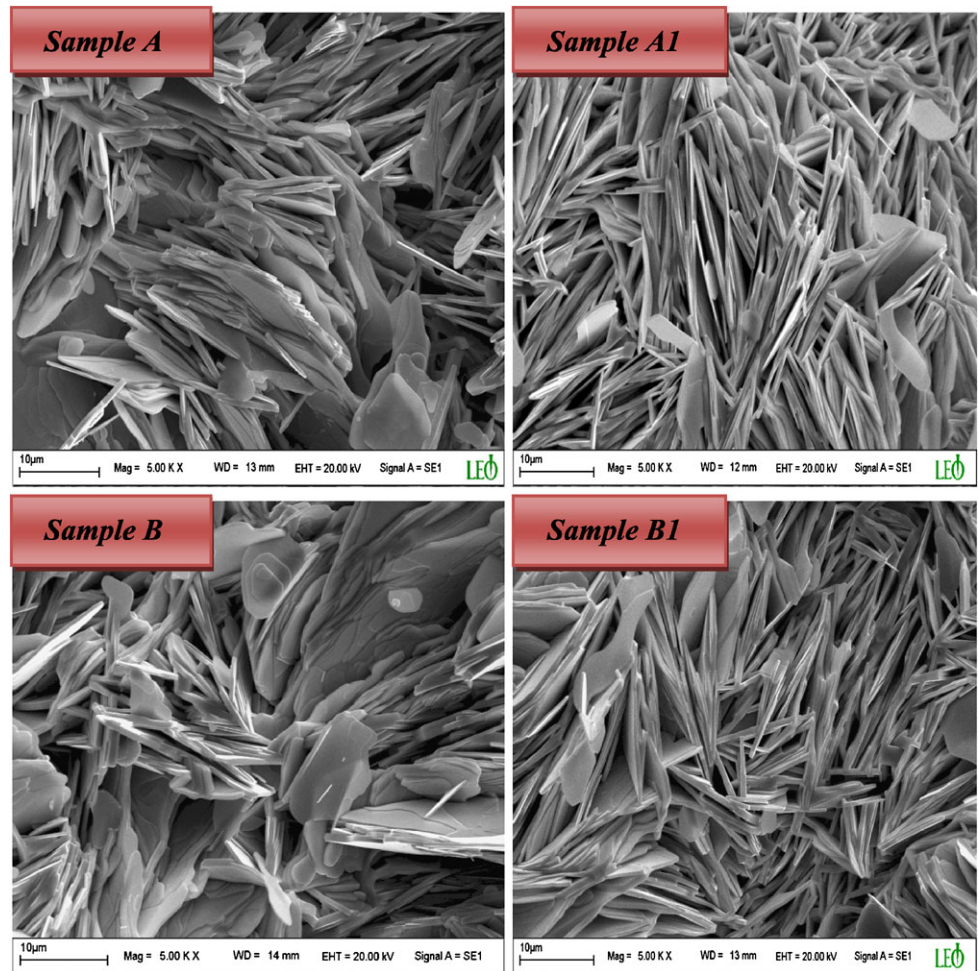**Fig. 2** (Color online) XRD patterns of samples *A*, *B*, *A1* and *B1*

Fig. 3 SEM photographs of sample *A*, *B*, *A1* and *B1*

phases, particularly the Ca$_2$PbO$_4$ unknown phase was detected. The unit-cell dimensions were determined from the observed d-spacing by a least squares method assuming the structure to be tetragonal with increasing Ti and sintering time. We have got the precise cell dimensions; $a = 5.41$ Å, $c = 30.78$ Å; $a = 5.41$ Å, $c = 30, 76$ Å; $a = 5.39$ Å, $c = 30.75$ Å and $a = 5.39$ Å, $c = 30.75$ Å for samples A, B, A1 and B1, respectively. With increasing Ti concentration and sintering time, a small variations were observed at the values of a- and c-parameters. From the result of the XRD patterns, it became clear that increasing the sintering time caused a decreased amount of the high-T_c phase and appeared impurity phase, compared with lower sintering time. Thus, it can be concluded that the volume fraction of the (2223) phase decreased with prolonged sintering.

The SEM photographs are illustrated in Fig. 3 for the different Ti doped samples. All the figures contain both needle shapes and grain structure. This supports our resistivity and XRD results which show that the (2223) and (2212) phases are present in our samples. Samples A and B have a more uniform surface with a dense alignment of grains. It is seen that the surface composition of samples A and B is closer to that of the Bi-(2212) phase. This is also confirmed by the XRD and resistivity measurements given above.

In order to estimate the J_{cmag} values of the samples from the magnetization measurements, the Bean's model [19] was used:

$$J_{cmag} = 20 \frac{\Delta M}{a(1 - a/3b)}$$

where J_{cmag} is the magnetization current density in amperes per square centimeter of a sample. $\Delta M = M_+ - M_-$ is measured in electromagnetic units per cubic centimeter, a and b $(a < b)$ are the dimensions in centimeters of the cross-section of the sample parallel to the applied field.

The calculated critical current densities of the samples as a function of the applied field, at a four different fixed temperatures are shown in Figs. 4, 5, 6 and 7, and tabulated in Table 1. As can be seen from figures and Table 1, the maximum value of J_{cmag} (4.3×10^4 A/cm^2) is obtained at 9 K for optimally treated sample and then decreases with increasing temperature. All the samples prepared show that the field dependence of J_{cmag} is strong even at 9 K. This kind of behavior can be explained in terms of weak grain connectivity and/or an increased volume fraction of impurity grains, such as formation of both (2212) and (2223) phases.

In general, higher values of J_c have been calculated while weak magnetic field dependence was still obtained at $T > 9$ K. This is expected because the magnetization curve of the sample forms a loop that indicates the presence of the pinning centers on the surface of the materials. It is also well known that in the high-T_c superconducting material non-superconducting impurity phases observed in the samples
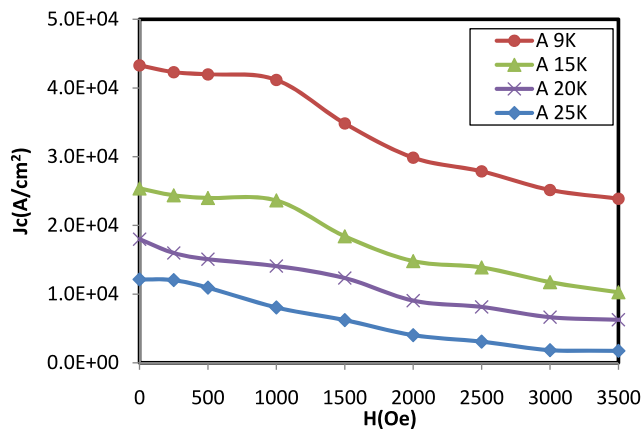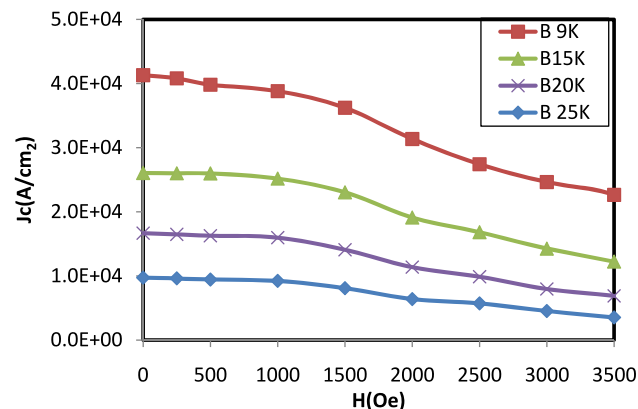

Fig. 4 J_{cmag} results of sample A
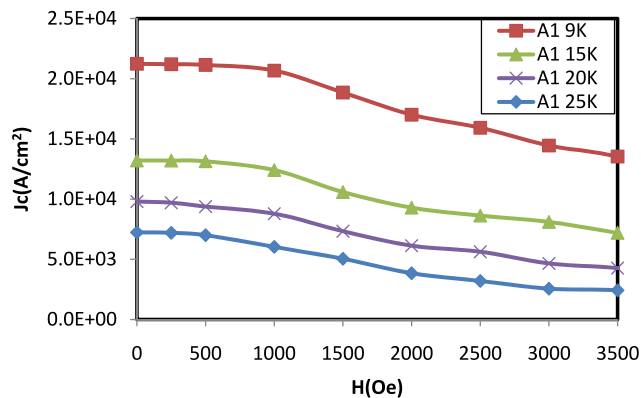

Fig. 5 J_{cmag} results of sample B

Fig. 6 J_{cmag} results of sample A1

sintered 192 hours are highly effective in the flux-pinning mechanism. Thus, a higher critical current density with a small amount of non-superconducting phases is possible.
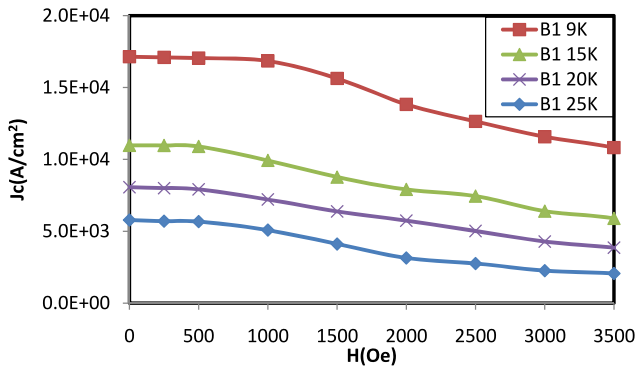
Fig. 7 J_{cmag} results of sample B1

Table 1 The critical current values of the samples

Sample name	J_{cmag} at 9 K (A/cm^2)	J_{cmag} at 15 K (A/cm^2)	J_{cmag} at 20 K (A/cm^2)	J_{cmag} at 25 K (A/cm^2)
A	4.3×10^4	2.6×10^4	1.8×10^4	1.2×10^4
A1	2.1×10^4	1.4×10^4	1.0×10^4	0.7×10^4
B	4.1×10^4	2.5×10^4	1.7×10^4	1.0×10^4
B1	1.7×10^4	1.1×10^4	0.8×10^4	0.6×10^4

4 Conclusion

The results presented above indicate that the sintering time plays very much role on the superconducting properties of the sample. From R–T results, although the (2223) phase seems as the dominant in A1 sample for the sintering time of 192 hours, but X-ray, SEM and magnetization results do not support this result. With increasing Ti and sintering time, the superconducting properties are depressed. The formation of a weak coupling between the impurities and grains produces a lower critical transition temperature. The critical current values of the samples sintered 185 hours are much higher than those of the samples sintered 192 hours.

References

1. Anderson, P.W.: Science **235**, 1196 (1987)
2. Ekicibil, A., Coşkun, A., Özçelik, B., Kiymaç, K.: *Modern Physics Letters B* 18(23), 1-12 (2004)
3. Özkurt, B., Ekicibil, A., Aksan, M.A., Özçelik, B., Yakıncı, M.E., Kiymaç, K.: J. Low Temp. Phys. **147**, 31 (2007)
4. Özkurt, B., Ekicibil, A., Aksan, M.A., Özçelik, B., Yakıncı, M.E., Kiymaç, K.: J. Low Temp. Phys. **149**, 105 (2007)
5. Tarascon, J.M., Barboux, P., Hull, G.W.: Phys. Rev. B **39**, 4316 (1989)
6. Jiang, J., Abell, J.J.: Supercond. Sci. Technol. **11**, 7005 (1998)
7. Singh, J.P., Jou, J., Vasanthamahan, N., Poeppel, R.B.: J. Mater. Res. **8**, 2458 (1993)
8. Chevalier, B., Lepine, B., Lalerzin, A., Darriet, J., Eournau, J., Tarascon, J.M.: Mater. Sci. Eng. B **2**, 277 (1989)
9. Chen, Y.L., Stevens, R.: J. Am. Ceram. Soc. **75**, 1150 (1992)
10. Sunshine, S.A., Siegrist, T., Schneemeyer, L.F., Murphy, D.W., Cava, R.J., Batlogg, B., van Dover, R.M., Fleming, R.M., Glarum, S.H., Nakahara, S., Farrow, R., Krajewski, J.J., Zahurak, S.M., Waszczak, J.V., Marshall, J.H., Marsh, P., Rupp, L.W. Jr., Peck, W.F.: Phys. Rev. B, Condens. Matter Mater. Phys. **38**(1), 893 (1988)
11. Ramesh, R., Green, S., Jiang, C., Mei, Y., Rudee, M., Luo, H., Thomas, G.: Phys. Rev. B, Condens. Matter Mater. Phys. **38**(10), 7070 (1988)
12. Kijima, N., Endo, N., Tsuchiya, J., Sumiyama, A., Mizino, M., Oguri, Y.: Jpn. J. Appl. Phys. **27**, L821 (1988)
13. Shi, D., Boley, M.S., Chen, J.G., Xu, M., Vandervoort, K., Liao, Y.X., Zangvil, A., Akujize, J., Segre, C.: Appl. Phys. Lett. **55**, 699 (1989)
14. Endo, U., Koyama, S., Kawai, T.: Jpn. J. Appl. Phys. **27**(8), L1476 (1988)
15. Tanaka, Y., Fukutomi, M., et al.: Jpn. J. Appl. Phys. **27**(4), L548 (1988)
16. Tallon, J.L., Buckley, R.G., Gilberd, P.W., Preland, M.R.: Physica C **158**, 247 (1989)
17. Sözeri, H., Ghazanfari, N., Özkan, H., Kılıç, A.: Supercod. Sci. Technol. **20**, 1 (2007)
18. Yazıcı, D.: Ph.D. thesis (2010)
19. Bean, C.P.: Phys. Rev. Lett. **8**, 250 (1962)